Supplemental material

Meyer et al., https://doi.org/10.1084/jem.20171312

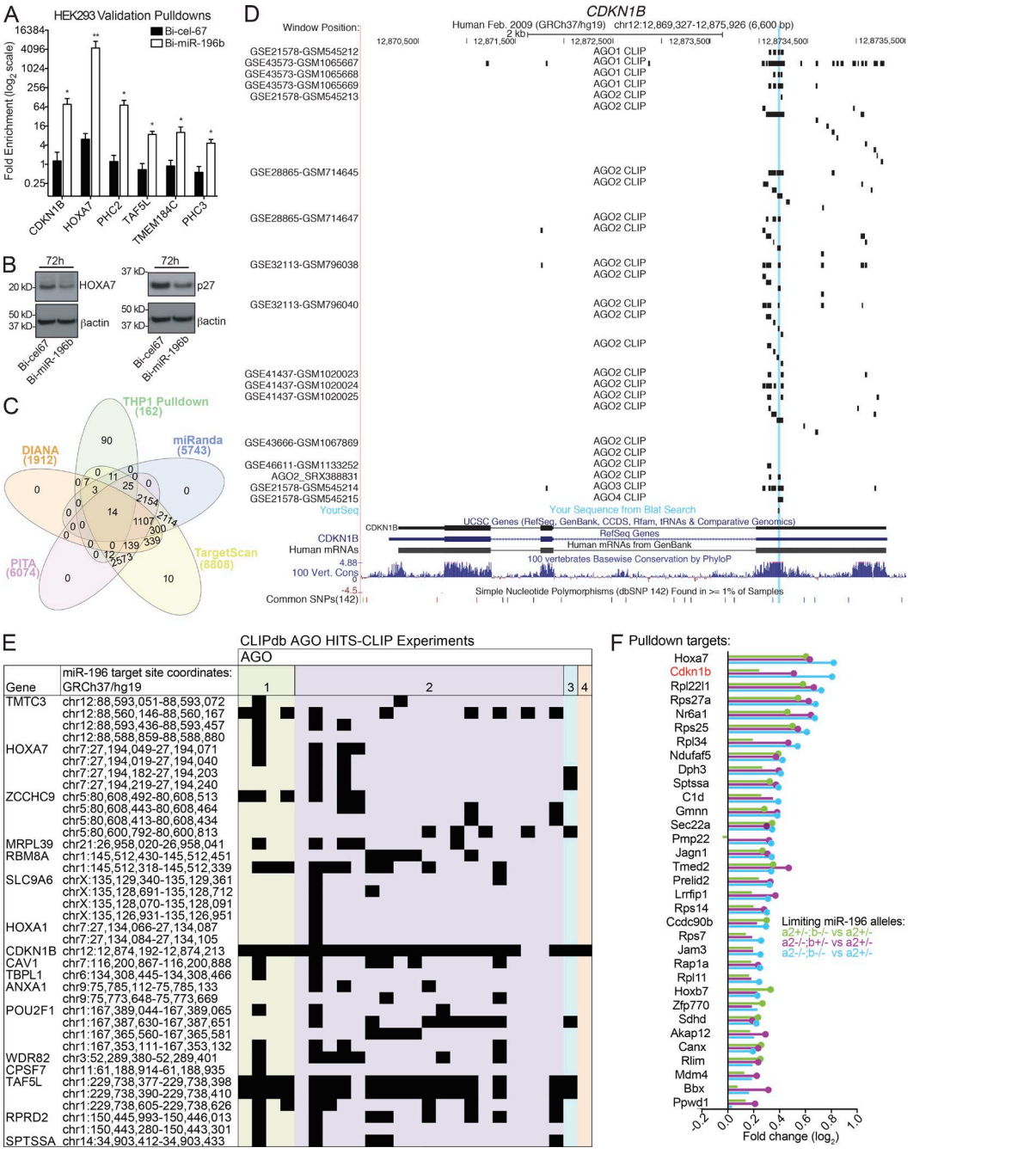

Figure S1. **Optimization, characterization, and corroboration of biotinylated miRNA mimic target pulldown approach. (A)** The average ± SEM fold pulldown by RT-qPCR relative to matched input controls for each Bi-cel-67 control (black bars) and Bi-miR-196b mimic (white bars) in three to four independent pulldowns in HEK293 cells. Statistical significance by paired *t* tests for each gene versus Bi-cel-67 control. Results shown are an average of at least three independent experiments. *, P ≤ 0.05; **, P ≤ 0.01. **(B)** Immunoblot analyses for known (HOXA7) and pulldown-identified (p27) miR-196b targets were performed on whole cell lysates from HEK293T cells transfected with indicated Bi-miR mimics (β-actin served as loading control). A representative of two independent experiments is shown. **(C)** Venn diagram of miR-196b pulldown targets in THP1 cells from Fig. 1 B, with target algorithm predicted miR-196b targets from four different algorithms: DIANA, miRanda, PITA, and TargetScan. **(D and E)** AGO CLIP sequencing data from CLIPdb[52] (Table S1) was manually searched using BLAT in UCSC Genome Browser for miR-196b binding sites in pulldown targets identified in human AML cells from Fig. 1 B. Example UCSC Genome Browser AGO CLIP tracks for pulldown target *CDKN1B* in D shows overlap of AGO binding with miR-196b target site (blue highlight). The process was repeated for several Bi-miR-196b pulldown targets, and the chart in E summarizes the results for each candidate miR-196b binding site (genomic coordinates). The AGO CLIP-Seq dataset(s) in CLIPdb with corresponding AGO binding site overlap are indicated for each (black squares). **(F)** Mouse orthologues of the top 500 target genes identified by biotinylated miR-196b pulldowns in human AML cells, were queried in quantitative gene expression datasets generated from E9.5 miR-196 mutant mouse embryos by RNA-seq. *miR-196a2*$^{+/-}$ control (n = 5) were compared with embryos with limiting alleles of miR-196 (*196a2*$^{+/-}$;*b*$^{-/-}$, *196a2*$^{-/-}$;*b*$^{+/-}$, or *196a2*$^{-/-}$;*b*$^{-/-}$ vs. *196a2*$^{+/-}$;*b*$^{+/+}$; n = 4/genotype). Genotype comparisons are color coded, filled circle at the tips of fold changes represent a statistically significant change at q < 0.05. Only genes that pass expression threshold requirements and exhibit significant up-regulated expression in at least one genotype comparison are displayed. *Cdkn1b* is highlighted (red) within this list.

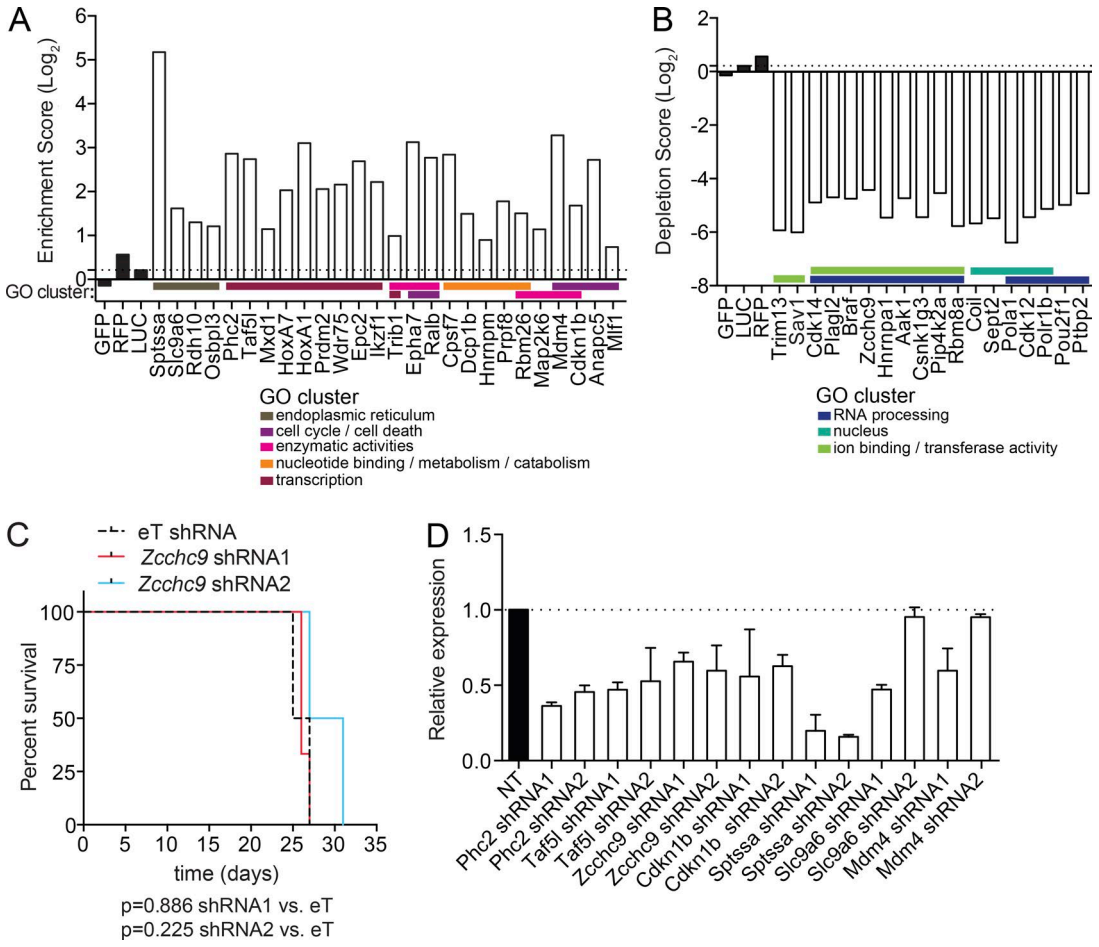

Figure S2. **shRNA knockdown of miR-196b pulldown targets in MLL-AF9 AML.** In vivo shRNA screening of AML-116 miR-196b pulldown targets was performed in murine MLL-AF9 leukemic splenocytes. **(A and B)** The average $\log_2$ RNAi screen enrichment (A) and depletion scores (B) of representative hairpins/gene within GO clusters compared with average hairpins/gene scores of three controls (GFP, LUC, and RFP; black bars). The dotted lines denote the average scores of control hairpins. **(C)** Survival curves of mice transplanted with MLL-AF9 leukemia cells expressing shRNA against *Zcchc9* or eT control (n = 3–4 mice/group). *Zcchc9* shRNA are a representative example of a gene whose hairpins were depleted from MLL-AF9 leukemia in the shRNA screen, and as anticipated, its knockdown does not accelerate leukemogenesis. No significant differences were detected between groups by Log-rank (Mantel-Cox) text. **(D)** shRNA activity was independently validated by TaqMan on leukemic splenocytes from at least two moribund mice each in Fig. 2 (D–G) and Fig. S2 C. *Sdha* served as a loading control, and shRNA-mediated knockdown is shown as relative to NT control mice for each gene. eT and LUC negative control shRNA showed similar gene expression as NT (data not shown).

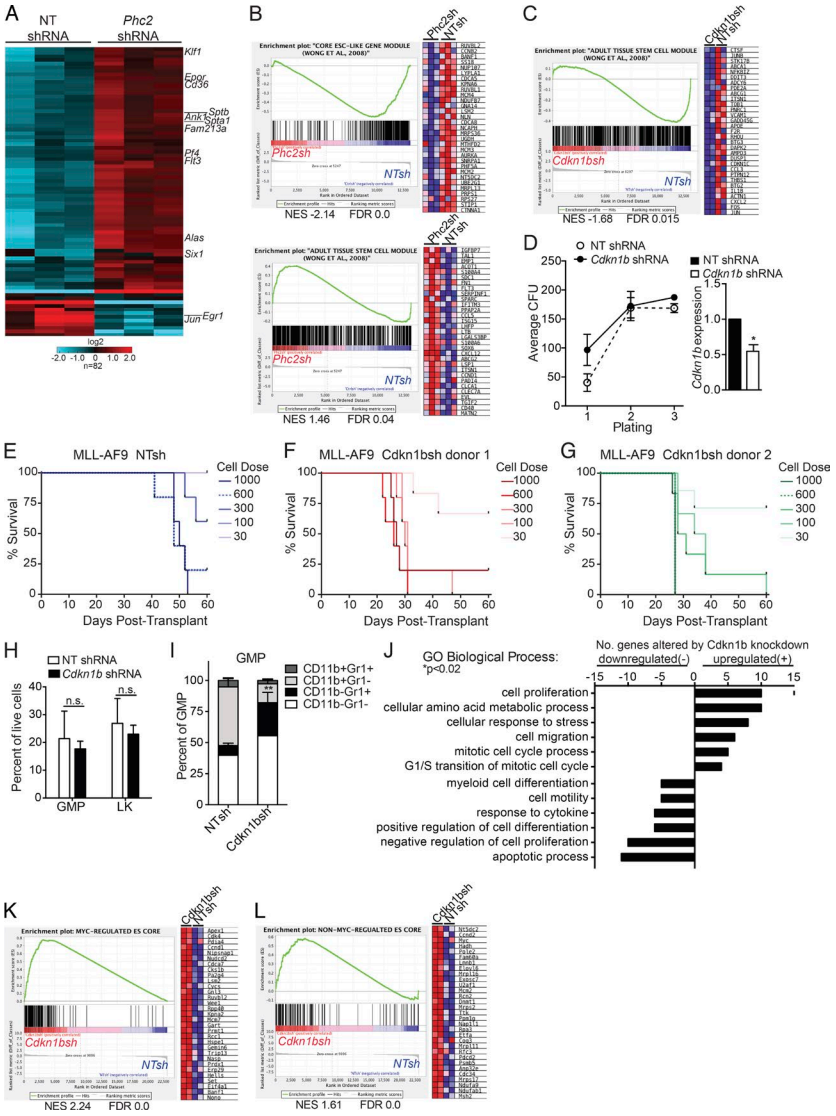

Figure S3. **Effects of *Cdkn1b* knockdown on MLL-AF9 transcriptional programming and immunophenotype. (A)** Heat map of $\log_2$ gene expression in *Phc2* shRNA-knockdown and NT control leukemias. Hierarchical clustering of 82 differentially expressed genes showing greater than twofold change in expression by RNA-Seq analysis of NT shRNA control ($n = 3$) or *Phc2* shRNA ($n = 3$) expressing MLL-AF9 leukemic splenocytes. **(B)** GSEA analyses plots ranking ESC core gene set (upper) and adult tissue stem cell gene set (lower) along descending fold change gene expression in *Phc2*-knockdown ($n = 3$ mice) versus NT control ($n = 3$ mice) MLL-AF9 leukemias by RNA-Seq. Expression of the top subset of leading edge genes in the *Phc2* shRNA (Phc2sh) or control NT shRNA (NTsh) MLL-AF9 leukemias is shown for each GSEA. NES, normalized enrichment score. **(C)** GSEA plot ranking adult tissue stem cell gene set along descending fold change gene expression in *Cdkn1b*-knockdown versus NT control leukemias by RNA-seq ($n = 2$ mice/group). Expression of the top subset of leading edge genes in the *Cdkn1b* shRNA (Cdkn1bsh) or control NT shRNA (NTsh) MLL-AF9 leukemias is shown for each GSEA. **(D)** MLL-AF9 leukemic splenocytes transduced with NT shRNA control or *Cdkn1b* shRNA lentiviruses, puromycin selected, and 3×10^3 cells/group were plated in methylcellulose colony forming assays (CFU). Left, average CFU ± SEM of NT (dashed line) or *Cdkn1b* (solid line) shRNA transduced MLL-AF9 cells performed in triplicate. Cells were replated in triplicate for a total of three platings. A representative of two independent experiments is shown. Two-way ANOVA Bonferroni's multiple comparisons test was used to evaluate statistical significance, no differences were detected. Right, RNA was isolated from NT or *Cdkn1b* shRNA MLL-AF9 cells after serial replating, and *Cdkn1b* expression measured by TaqMan. Two technical replicates are shown as representative of at least two independent experiments with similar results. *Sdha* served as a loading control and expression is shown relative to NT control. *, $P \le 0.05$ by *t* test. **(E–G)** Survival curves of mice ($n = 6$/cell dose per shRNA) transplanted with the indicated number of NTsh (E), Cdkn1bsh donor 1 (F), or Cdkn1bsh donor 2 (G) MLL-AF9 AML cells. **(H and I)** Leukemic splenocytes harvested from moribund NT shRNA control and *Cdkn1b*-knockdown mice were evaluated by flow cytometric analyses for differences in progenitor gate populations LK and GMP (H) and myeloid differentiation markers CD11b and Gr1 on leukemic GMP-gate cells (I). The average percentages of the indicated populations ± SEM are shown ($n = 3$/group). Statistically significant differences between NT shRNA and *Cdkn1b* shRNA groups were evaluated by *t* test for LK, GMP-gate in H, and two-way ANOVA Bonferroni's multiple comparisons test was used to determine significant differences between NT and *Cdkn1b* shRNA groups for each population in I. **, $P \le 0.01$. n.s., not significant. **(J)** Gene ontology analyses of differentially expressed genes from RNA-Seq analyses of *Cdkn1b*-knockdown MLL-AF9 leukemia cells compared with NT control ($n = 2$ mice/group; Fig. 3 A). GO biological processes are reported as a bar graph showing the number of up-regulated (+) or down-regulated (–) genes. **(K and L)** GSEA analyses plots ranking along descending fold change gene expression in *Cdkn1b*-knockdown MLL-AF9 cells compared with NTsh MLL-AF9 control ($n = 2$ mice/group). Gene sets were derived from the Wong ESC core gene set (from Fig. 3 B) divided into two groups: Myc-regulated target genes (K) or non–Myc-regulated target genes (L). Expression of the top subset of leading edge genes is shown for each GSEA.

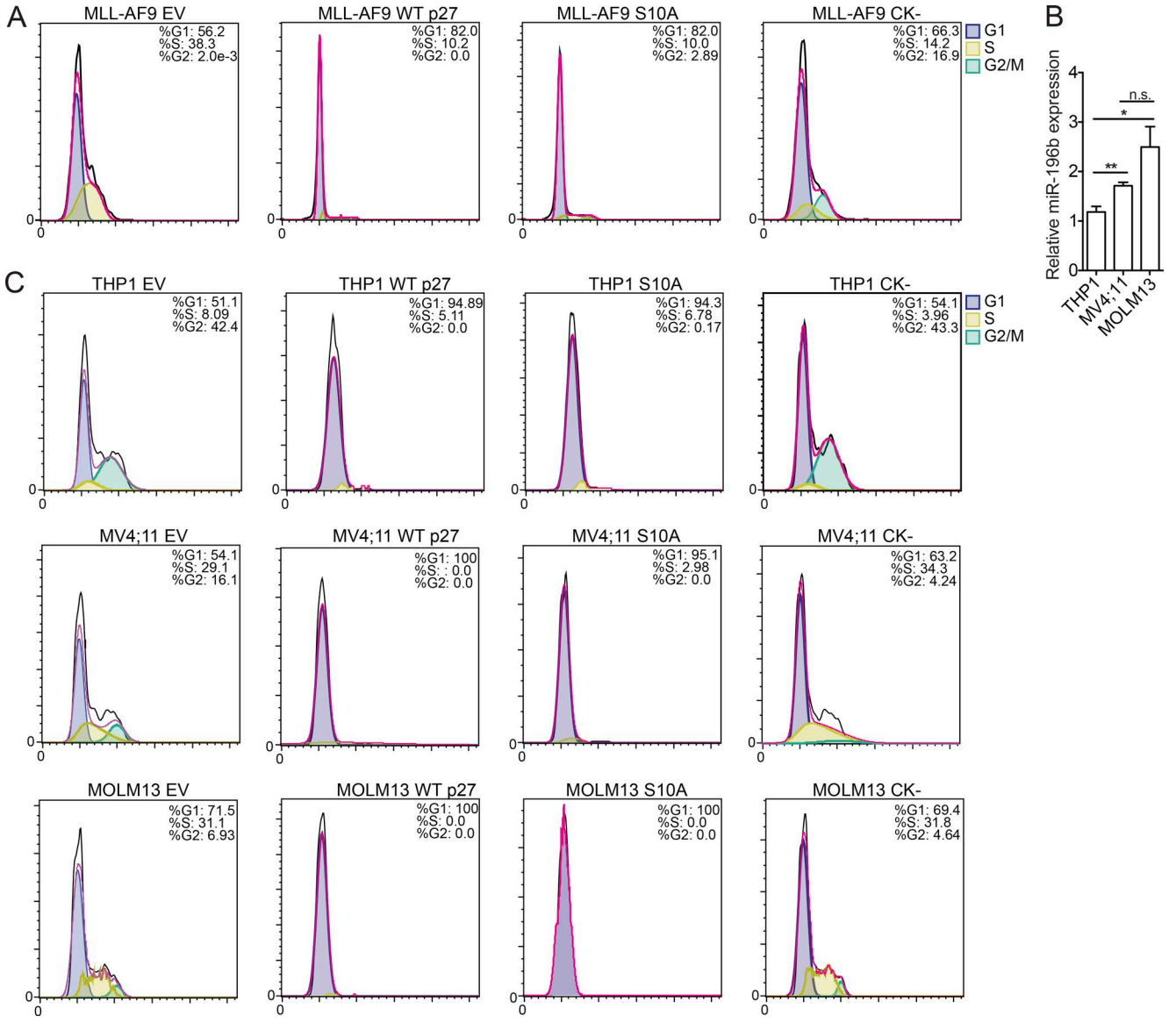

Figure S4. **p27^{Kip1} induces cyclin/cdk-dependent cell cycle arrest in MLL-r AML. (A)** Representative histograms of Vybrant DyeCycle DNA dye stained ZsGreen^{+} murine MLL-AF9 cells at 48 h after transduction with EV, WT p27, S10A, and CK^{-} lentiviruses. Areas used to calculate the percentage of cells in each cell cycle stage are indicated for G1 (purple), S (yellow), and G2/M (green). The percent of cells per cell cycle stage are indicated in the upper right corner of each histogram. The experiment was repeated at least twice with similar results. **(B)** Average relative expression of miR-196b ± SEM by RT-qPCR analyses of RNA isolated from human AML cell lines THP1, MV4;11, and MOLM13. Results are average of two independent experiments. Significant differences were evaluated by parametric unpaired *t* tests. *, P ≤ 0.05; **, P ≤ 0.01. n.s., not significant. **(C)** Representative histograms of Vybrant DyeCycle DNA dye stained ZsGreen^{+} THP1, MV4;11, and MOLM13 cells at 48 h post-transduction with EV, WT p27, S10A, or CK^{-} lentiviruses. Areas used to calculate the percentage of cells in each cell cycle stage are indicated for G1 (purple), S (yellow), and G2/M (green). The percent of cells per cell cycle stage are indicated in the upper right corner of each histogram. The experiment was repeated at least twice with similar results.

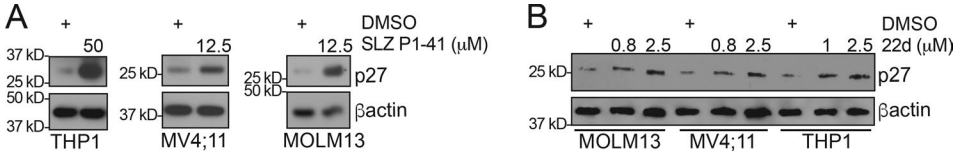

Figure S5. **p27^{Kip1} levels in human AML treated with SCF^{Skp2} inhibitors.** Immunoblots for p27 and loading control β-actin on protein lysates generated from THP1, MV4;11, and MOLM13 human AML cells after 24 h treatment with SLZ P1-41 (A) or 22d (B). SLZ P1-41 doses chosen for immunoblot were based on the lowest dose to achieve a significant reduction in cell viability as indicated by black arrows in Fig. 5 B. 22d doses were chosen based on mid and high used in synergy assays in Fig. 5 (C–E). A representative of two independent experiments is shown.

Tables S1, S2, and S3 are included as separate Excel files. Table S1 shows AGO-CLIP-Seq datasets from CLIPdb. Table S2 shows differentially expressed genes in Cdkn1b shRNA expressing MLL-AF9 AML compared with NT shRNA control AML. Table S3 presents Skp2 inhibitor 22d synergy drug analyses in combination with I-BET151, MI-1, or Palbociclib.

References

Agarwal, V., G.W. Bell, J.W. Nam, and D.P. Bartel. 2015. Predicting effective microRNA target sites in mammalian mRNAs. *eLife*. 4:e05005. https://doi.org/10.7554/eLife.05005

Betel, D., M. Wilson, A. Gabow, D.S. Marks, and C. Sander. 2008. The microRNA.org resource: targets and expression. *Nucleic Acids Res*. 36(Database):D149–D153. https://doi.org/10.1093/nar/gkm995

Enright, A.J., B. John, U. Gaul, T. Tuschl, C. Sander, and D.S. Marks. 2003. MicroRNA targets in Drosophila. *Genome Biol*. 5:R1. https://doi.org/10.1186/gb-2003-5-1-r1

John, B., A.J. Enright, A. Aravin, T. Tuschl, C. Sander, and D.S. Marks. 2004. Human MicroRNA targets. *PLoS Biol*. 2:e363. https://doi.org/10.1371/journal.pbio.0020363

Kim, J., J. Chu, X. Shen, J. Wang, and S.H. Orkin. 2008. An extended transcriptional network for pluripotency of embryonic stem cells. *Cell*. 132:1049–1061. https://doi.org/10.1016/j.cell.2008.02.039

Kim, J., A.J. Woo, J. Chu, J.W. Snow, Y. Fujiwara, C.G. Kim, A.B. Cantor, and S.H. Orkin. 2010. A Myc network accounts for similarities between embryonic stem and cancer cell transcription programs. ***Cell***. 143:313–324. https://doi.org/10.1016/j.cell.2010.09.010

Lewis, B.P., I.H. Shih, M.W. Jones-Rhoades, D.P. Bartel, and C.B. Burge. 2003. Prediction of mammalian microRNA targets. *Cell*. 115:787–798. https://doi.org/10.1016/S0092-8674(03)01018-3

Lewis, B.P., C.B. Burge, and D.P. Bartel. 2005. Conserved seed pairing, often flanked by adenosines, indicates that thousands of human genes are microRNA targets. *Cell*. 120:15–20. https://doi.org/10.1016/j.cell.2004.12.035

Maragkakis, M., M. Reczko, V.A. Simossis, P. Alexiou, G.L. Papadopoulos, T. Dalamagas, G. Giannopoulos, G. Goumas, E. Koukis, K. Kourtis, et al. 2009b. DIANA-microT web server: elucidating microRNA functions through target prediction. *Nucleic Acids Res*. 37(Web Server):W273-276. https://doi.org/10.1093/nar/gkp292

Papadopoulos, G.L., P. Alexiou, M. Maragkakis, M. Reczko, and A.G. Hatzigeorgiou. 2009. DIANA-mirPath: Integrating human and mouse microRNAs in pathways. *Bioinformatics*. 25:1991–1993. https://doi.org/10.1093/bioinformatics/btp299

Somervaille, T.C., and M.L. Cleary. 2006. Identification and characterization of leukemia stem cells in murine MLL-AF9 acute myeloid leukemia. *Cancer Cell*. 10:257–268. https://doi.org/10.1016/j.ccr.2006.08.020